

1. Introduction

The concept of elementary modes of excitation originated by Landau ¹⁾ has been central in the realization that many-body problems are amenable to a rigorous mathematical treatment exploiting the methods of quantum field theory.

Frölich ²⁾ and Pines ³⁾ started such a program in the field of solid state physics, a program which has developed into a whole new discipline, while Kohn and Luttinger ⁴⁾ and the Russian school ⁵⁾ provided the basic rigorous proofs of the ideas of elementary excitations.

The concept of elementary excitations and their mutual interplay was introduced in the realm of nuclear physics by Bohr and Mottelson to obtain a unified picture of nuclear structure ⁶⁾, and later developed into a field theory – the nuclear field theory (NFT) – based on the particle-vibration coupling mechanism [cf. refs. ⁶⁻⁹⁾].

The basic elementary modes of excitation which can be viewed as building blocks of the nuclear spectrum are (a) single-particle states ¹⁰⁾, (b) shape, spin and isospin vibrations ⁶⁾ and surface rotations ¹¹⁾, and (c) pairing rotations and pairing vibrations ^{12, 13)}.

In recent years it has been suggested [cf. refs. ¹⁴⁻¹⁷⁾] that the basic building blocks of the low-energy nuclear spectrum are pairs of fermions coupled to angular momentum zero and two.

To make contact with the approach of refs. ⁶⁻⁹⁾, the IBM model was recast in the framework of the NFT ^{18, 19)}. For this, the s- and d-bosons were assumed to be monopole and quadrupole pairing vibrations, and the graphs which in the microscopic description give the effective interaction between the bosons proposed by the IBM, were identified. They correspond to all the $1/\Omega$ two-phonon interactions between the pairing modes, plus some $1/\Omega^2$ renormalizing graphs, which take into account the coupling of the quadrupole pairing modes with the monopole condensate.

For the case of only s-bosons, the approximation gives, for a single j -shell, the exact answer ²⁰⁾. For many particles moving in a single j -shell, and interacting via monopole and quadrupole pairing forces, the IBM wave function seems to be a reasonable approximation to the exact solution for harmonic and transitional spectra ^{21, 22)}. However, for strongly deformed systems, Bohr and Mottelson have shown ²³⁾ in a schematic model that the IBM wave function is rather different from the exact solution of the problem (aligned wave function) [cf. also refs. ^{24, 25)}].

In an attempt to understand how these differences reveal themselves in the different properties of the low-energy nuclear spectrum, we have carried out microscopic pair-aligned calculations, within the framework of the NFT, and compared the results to experiment. The calculations were performed for the Kr isotopes, which are examples of typical anharmonic systems, and for the Sm isotopes, which provide a good example of rotation-vibration phase transition [†].

[†] It is noted that the spectrum of the Kr and that of the Sm isotopes have already been calculated utilizing the IBM and are reported in the literature ^{26, 27)}. The calculations presented here are however microscopic.

In sect. 2 we present the basic details of the model and of the parameters and in sects. 3 and 4 the results for the Kr and Sm isotopes respectively. The conclusions are presented in sect. 5.

2. The model

The particles move in a single j -shell and interact through a multipole ($\lambda = 0, 2$) pairing force and through a quadrupole particle-hole interaction. The multipole pairing hamiltonian is defined as in ref. ⁹⁾ and reads

$$H_p(\lambda) = -G_\lambda(2\lambda + 1) \sum_{\lambda\mu} P_{\lambda\mu}^+ P_{\lambda\mu}, \quad (1)$$

where, for a single j -shell,

$$P_{\lambda\mu}^+ = \left(\frac{2\pi}{2\lambda + 1} \right)^{\frac{1}{2}} \langle j || T_\lambda || j \rangle [c_j^+ c_j^+]_{\lambda\mu} / \sqrt{2}. \quad (2)$$

From a systematic analysis of the nuclear spectrum [cf. e.g. ref. ²⁸⁾] it has been found, utilizing $T_{\lambda\mu} = Y_{\lambda\mu}$, that $G \sim 27/A$ MeV independent of λ ($\lambda = 0, 2$ and 4).

The s - and d - bosons of the pair-aligned model are here interpreted as monopole and quadrupole pairing vibrations. For a single j -shell, the RPA relation which determines the energy W_λ of the multipole pairing vibrations reduce to

$$\varepsilon - W_\lambda = 2\pi G_\lambda \langle j || T_\lambda || j \rangle^2. \quad (3)$$

The quantity

$$Z_\lambda = \varepsilon - W_\lambda \quad (4)$$

is the correlation energy associated with the mode, ε being twice the energy of the j -shell where the particles correlate. From systematics one obtains $Z_0 \sim 1.5$ MeV and $Z_2 \sim 0.5$ MeV.

The RPA amplitude associated with the mode λ is

$$d = 1 = - \frac{A_\lambda}{\sqrt{2}} \frac{\langle j || T_\lambda || j \rangle}{\varepsilon - W_\lambda} \quad (5)$$

The particle-vibration coupling strength is given by

$$\sqrt{2} Z_\lambda = -A_\lambda \langle j || T_\lambda || j \rangle, \quad (6)$$

and measures the strength with which the particle couples to the pairing modes.

The monopole and quadrupole pairing vibrations interact through a quadrupole particle-hole force

$$H_Q = - \sum_{t_{z_1} t_{z_2}} K(t_{z_1} t_{z_2}) \sum_{\mu} (-1)^\mu Q_{2\mu} Q_{2-\mu}. \quad (7)$$

This force has an isoscalar and an isovector component. The self-consistent values of the corresponding strengths [cf. refs. ^{6, 29}] are

$$K \equiv K(\tau=0) \approx \frac{120}{A^{5/3}} \left(\frac{M\omega_0}{\hbar} \right)^2 \text{ MeV}, \quad (8)$$

and

$$b = -\frac{K(\tau=1)}{K(\tau=0)} \approx -1.5 \frac{V_1}{V_2}. \quad (9)$$

The quantities V_0 and V_1 are the isoscalar and isovector shell model potentials. Utilizing $V_0 = -50$ MeV and $V_1 = 120$ MeV, one obtains $b = 3.6$. Thus, the bare interaction strength is given by [cf. ref. ²⁹]

$$K_{\text{bare}}(t_{Z_1}, t_{Z_2}) \approx K(1 - 4t_{Z_1} t_{Z_2} b). \quad (10)$$

A quadrupole force will induce, for particles moving in a harmonic oscillator, particle-hole excitations of $\Delta N = 0$ and $\Delta N = 2$ type, N being the harmonic oscillator principal quantum number.

The low-lying modes are essentially built out of $\Delta N = 0$ excitations, while the giant resonances are mainly based on the $\Delta N = 2$ particle-hole excitations.

Setting to zero the spin-orbit term in the single-particle potential, one obtains a schematic model of the quadrupole response function which can be solved analytically. In this case the $\Delta N = 0$ excitations have zero energy, and the full response function is exhausted by the isoscalar and isovector giant resonances ($\Delta N = 2$ modes) which have an energy given by

$$E(\tau) \approx \begin{cases} \sqrt{2}\hbar\omega_0 & (\tau = 0) \\ \sqrt{11}\hbar\omega_0 & (\tau = 1). \end{cases} \quad (11)$$

The quadrupole effective interaction arising from the exchange of the quadrupole modes is, in this model, given by[†] [cf. also ref. ³⁰]

$$\frac{K_{\text{eff}}(t_{Z_1}, t_{Z_2})}{K} \approx \begin{cases} 4 \frac{1+b}{2+b} \approx 3.3 & (t_{Z_1} = \pm \frac{1}{2}, t_{Z_2} = \mp \frac{1}{2}) \\ \frac{4}{2+b} \approx 0.7 & (t_{Z_1} = \pm \frac{1}{2}, t_{Z_2} = \pm \frac{1}{2}) \end{cases} \quad (12)$$

As a bonus one gets from these estimates the effective charges

$$\frac{e_{\text{eff}}(\Delta N = 2; t_Z)}{e} = \begin{cases} 1 + \frac{1}{2+b} \approx 1.2 & (t_Z = -\frac{1}{2}) \\ \frac{1+b}{2+b} \approx 0.8 & (t_Z = \frac{1}{2}). \end{cases} \quad (13)$$

[†] For simplicity, the effect of the neutron excess has been neglected.

For a realistic single-particle potential both low-lying collective and giant resonances carry a sizable fraction of the energy-weighted sum rule. The effective quadrupole force resulting from the exchange of the quadrupole (both $\Delta N = 0$ and $\Delta N = 2$ in this case) is [cf. table 4.3, ref. ²⁹].

$$\frac{K(t_{Z_1}, t_{Z_2})}{K} \approx \begin{cases} 4 & (t_{Z_1} = \pm \frac{1}{2}, t_{Z_2} = \mp \frac{1}{2}) \\ 2 & (t_{Z_1} = \pm \frac{1}{2}, t_{Z_2} = \pm \frac{1}{2}). \end{cases} \quad (14)$$

The strength to be utilized lies somewhere between the estimates (12) and (14). In each specific case it is however easy to carry out the detailed renormalization.

3. The Kr isotopes

The calculations have been carried out utilizing both proton and neutron pairing modes. They were obtained by allowing the valence particles to move in a $j = \frac{3}{2}$ shell, corresponding to the degeneracy between the closed shells at nucleon numbers 28 and 50.

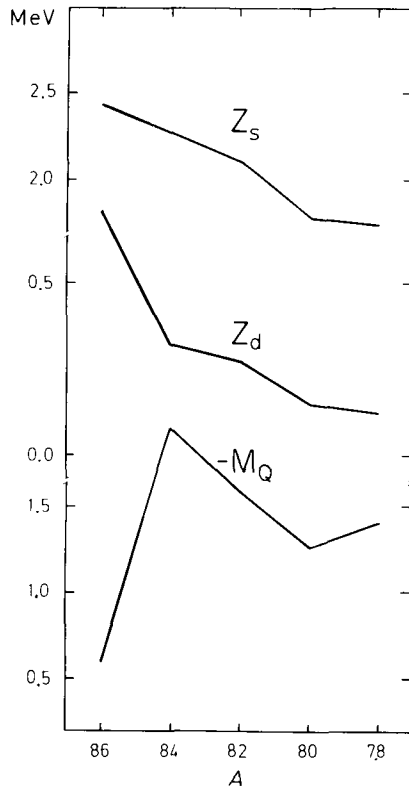


Fig. 1. Value of the parameters Z_s , Z_d and $-M_Q$ utilized in the calculation for the different Kr isotopes.

The basis states contain four proton-particle bosons and from 0 to 4 neutron-hole bosons. Already with such a small subspace, the matrices to be constructed are of the order of 200×200 (^{78}Kr).

The values of the parameters utilized in the calculation are displayed in fig. 1. The quadrupole force was chosen, according to (12), as

$$K(\frac{1}{2}, -\frac{1}{2}) = 4K(\frac{1}{2}, \frac{1}{2}) = 4K(-\frac{1}{2}, -\frac{1}{2}). \quad (15)$$

Utilizing the definitions of the previous section we can write, for a typical quadrupole matrix element

$$M_Q = -K(t_{z_1}, t_{z_2})Q^2, \quad (16)$$

where

$$Q \approx \langle jm|r^2 Y_{20}|jm\rangle \sim \sqrt{\frac{5}{4\pi}} \langle jm20|jm\rangle \langle j\frac{1}{2}20|j\frac{1}{2}\rangle \langle r^2\rangle \sim -\frac{1}{4}(N + \frac{3}{2}) \frac{\hbar}{M\omega_0}, \quad (17)$$

and

$$K(t_{z_1}, t_{z_2}) \sim \alpha \frac{\left[\frac{1}{4} \left[\binom{n_v}{2} + \binom{n_\pi}{2} \right] + \binom{n_{v\pi}}{2} \right]}{\left(\binom{n_v}{2} + \binom{n_\pi}{2} + \binom{n_{v\pi}}{2} \right)}. \quad (18)$$

the value of the quantity in brackets is, for the Kr isotopes, ~ 0.61 . For $A = 80$ and $N = 3$, one obtains

$$M_Q \sim -\alpha \times 0.1 \text{ MeV} \quad (19)$$

The average value of M_Q needed to fit the spectra of the $^{80}, ^{82}, ^{84}\text{Kr}$ isotopes is -1.6 MeV , which leads to a renormalization factor $\alpha \sim 16$. This number is to be compared with the estimate

$$\frac{K(\Delta N = 2; \tau = 0 + 1)}{K} \sim 4 \frac{1+b}{2+b} \sim 3.3. \quad (20)$$

One is thus left with a factor of the order of 5 unaccounted for. The need to use quadrupole matrix elements which are considerably larger than those obtained making use of the self-consistent value (8) of the quadrupole strength, seems to be due to the use of a single j -orbital, instead of a non-degenerate many j -shell configuration space [cf. ref. ²⁵].

The small value of M_Q for ^{86}Kr just reflects the factor of four existing between $K(\frac{1}{2}, -\frac{1}{2})$ and $K(\frac{1}{2}, \frac{1}{2})$. Thus, in the case $n_v = n_{v\pi} = 0$, relation (19) reads

$$M_Q \sim \alpha \times \frac{1}{4} \times 0.16 \text{ MeV}.$$

Utilizing the value of the matrix element of $\sim 0.5 \text{ MeV}$, we obtain $\alpha \sim 10$. Taking into account that about a factor of 5 is due to the use of a single j -shell, we are left

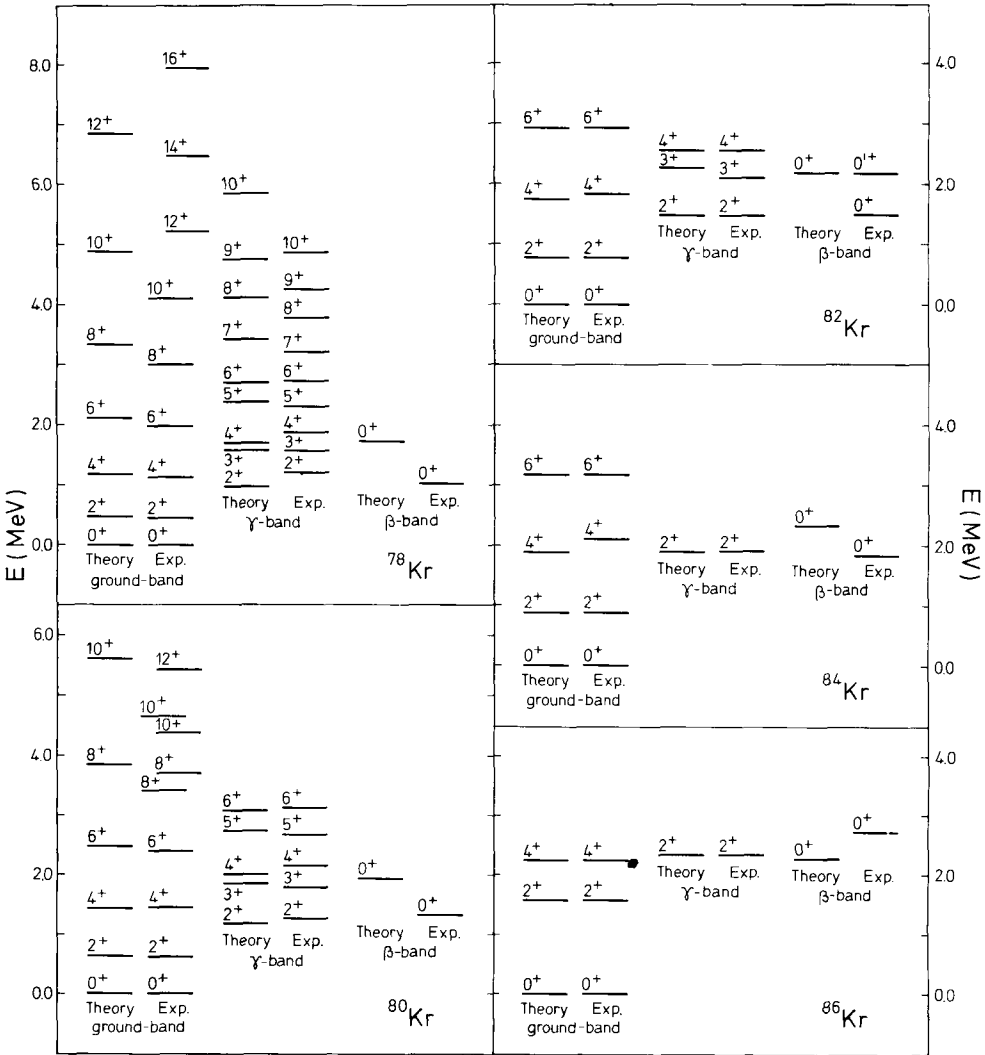


Fig. 2. Theoretical and experimental energy levels for the different Kr isotopes. The parameters used in the calculation are plotted in fig. 1.

with a renormalization factor of the order of 2, which is close to the estimate quoted in (14) for $t_{z_1} = \pm \frac{1}{2}$ and $t_{z_2} = \pm \frac{1}{2}$.

The spectrum associated with the different isotopes is shown in fig. 2, in comparison with the experimental data. The grouping of levels in bands is done on the basis of the wave functions. Examples are displayed in fig. 3. It is noted that a similar spectrum is obtained utilizing a single set of parameters i.e. $Z_s = 2.0$ MeV, $Z_d = 0.4$ MeV and $M_Q = -1.6$ MeV.

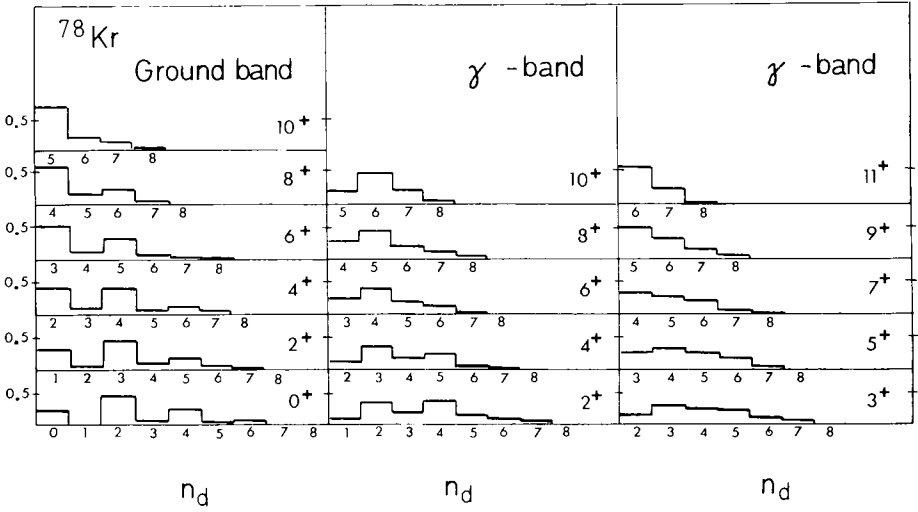


Fig. 3. Anatomy of the wave functions of the ground and γ -band of ^{78}Kr according to the components with different number of d-bosons.

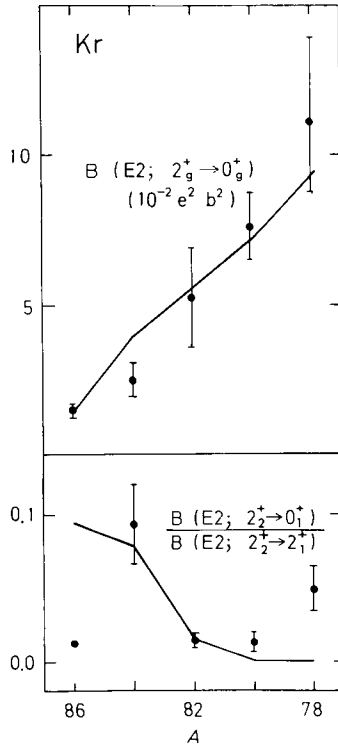


Fig. 4. Theoretical and experimental $B(E2)$ values for the first 2^+ state and branching ratios for the second 2^+ state for the different Kr isotopes.

The model provides with a good fitting to the ground-state rotational band. Concerning the γ -band the predicted moment of inertia is much smaller than experimentally observed, and the splitting between even and odd members (i.e. $3^+ - 4^+$, $5^+ - 6^+$, etc.) are too small. It is noted that these states are degenerate in the vibrational limit. The model thus predicts a quasi γ -band which is too close to the spherical limit.

Concerning the β -band, the model predicts a state which is much too high in energy. This is, maybe, because the model lacks the pairing vibration degree of freedom, and thus the coupling which can bring down the mainly β -vibrational state (cf. next section). Also, because of the averaging the model does over the shell structure.

The calculated electromagnetic transition amplitudes for the first and second 2^+ states are shown in fig. 4, for the various isotopes. The experimental patterns are fairly well reproduced.

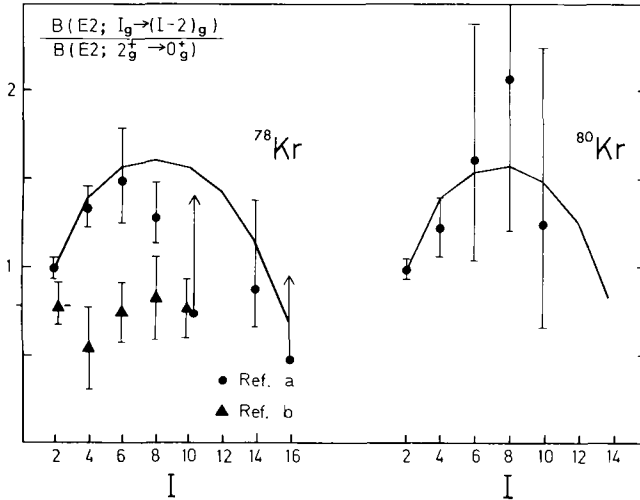


Fig. 5. Theoretical and experimental $B(E2; I+2 \rightarrow I)/B(E2; 2^+ \rightarrow 0_{g.s.}^+)$ ratios for the members of the yrast line in ^{78}Kr and ^{80}Kr . Experimental points from H. P. Hellmeister *et al.*, Nucl. Phys. **A332** (1979) 241 [ref. ^a] and R. L. Robinson *et al.*, Phys. Rev. **21C** (1980) 603 [ref. ^b]. A reduction of the $B(E2)$ strength at high angular momentum similar to the one reported in ref. ^a) has also been seen in the neighbour ^{79}Rb (J. Panqueva *et al.*, Phys. Lett. **98B** (1981) 248).

The $R = B(E2; I+2 \rightarrow I)/B(E2; 2 \rightarrow \text{g.s.})$ ratios for the members of the yrast line are shown in fig. 5 for ^{78}Kr and ^{80}Kr . Because of the finite model subspace, there is a rather strong limitation of the maximum angular momentum the nucleus can have, as compared to the shell-model prediction. For example, $I_{\text{max}} = 16$ for ^{78}Kr , which corresponds to the total alignment of 8 d-bosons. Due to this artificial cut-off, predictions beyond $I \sim 8$ are affected by the imposed limitations. The decrease of the ratio R reflects in fact this limitation and not the depletion of a degree of freedom[†].

[†] Concerning this point, we refer, e.g., to the Coulomb excitation study of ^{238}U [ref. ³¹].

4. The Sm isotopes

In this calculation, no distinction is made between neutrons and protons, and it is thus essentially the same as that reported in ref. ²⁷⁾ [cf. also ref. ³²⁾]. All particles outside the $Z = 50$ and the $N = 82$ closed shells are explicitly considered. They move in a single j -shell with degeneracy $\Omega = 38$.

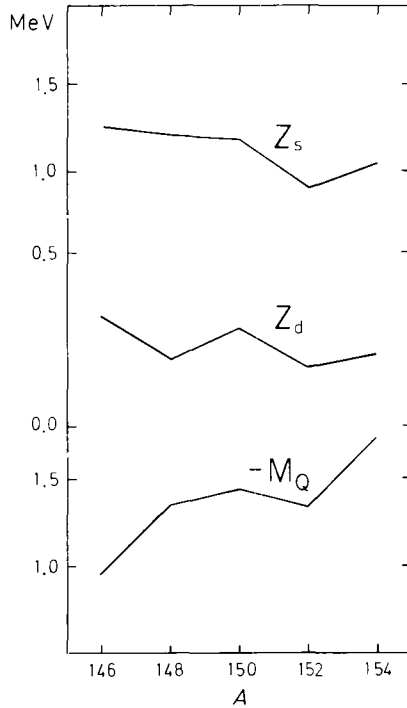


Fig. 6. Value of the parameters Z_s , Z_d and $-M_Q$ utilized in the calculation for the different Sm isotopes.

The parameters of the calculation resulting from a fitting of the data are shown in fig. 6. Had we taken constant parameters the quality of the fitting would not have been in any essential way altered. The predicted spectra in comparison with the experimental data are shown in fig. 7.

The phase transition is clearly accounted for. However, the moment of inertia of both the quasi- β and quasi- γ bands are, for ^{150}Sm and ^{152}Sm , about 50 % smaller than the experimental values, the predicted bands being still too vibrational. The change in the coupling scheme taking place through the Sm isotopes is further evidenced by the behaviour of the different electromagnetic transition probabilities shown in fig. 8.

An interesting insight into the meaning of the phase transition is obtained by looking at the wave functions of the low-lying states [cf. fig. 9; cf. also ref. ¹⁴⁾].

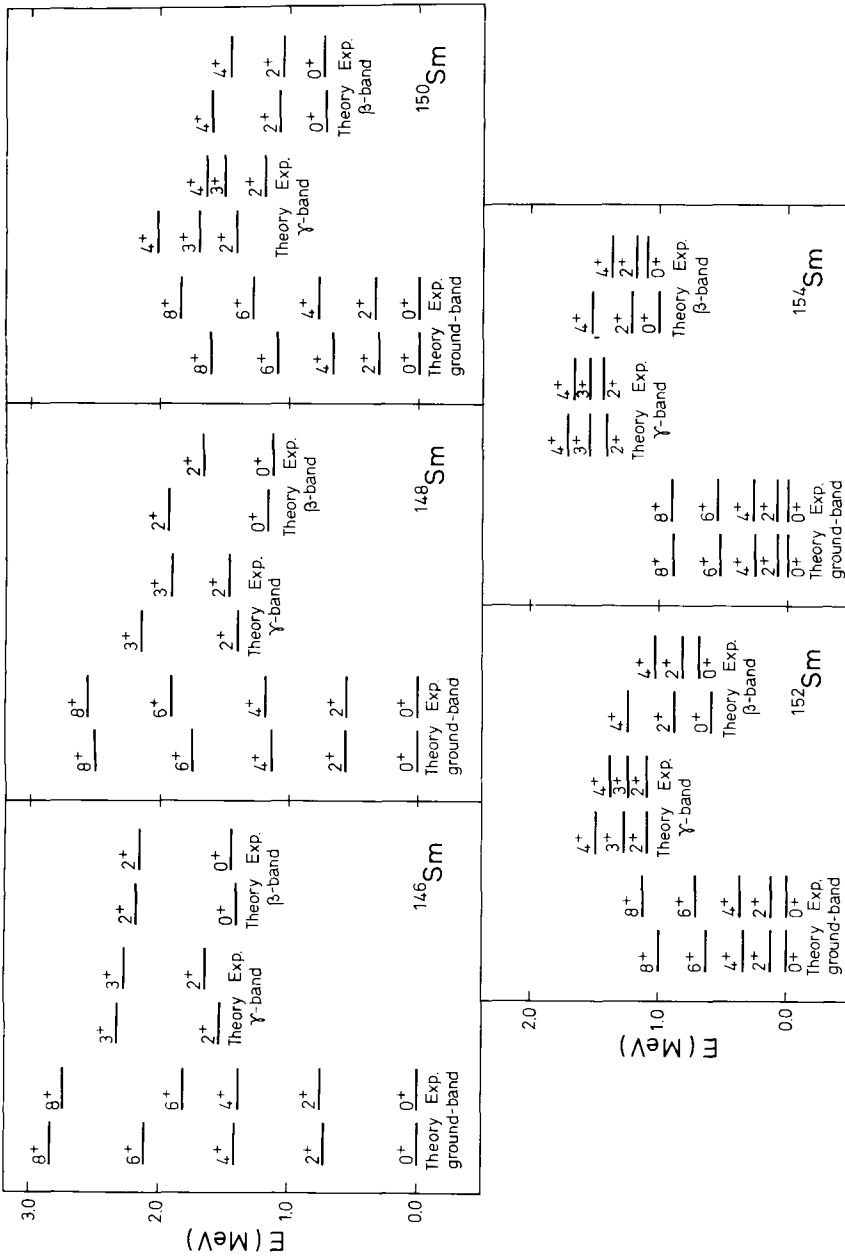


Fig. 7. Theoretical and experimental energy levels for the different Sm isotopes. The parameter used in the calculation are plotted in fig. 6.

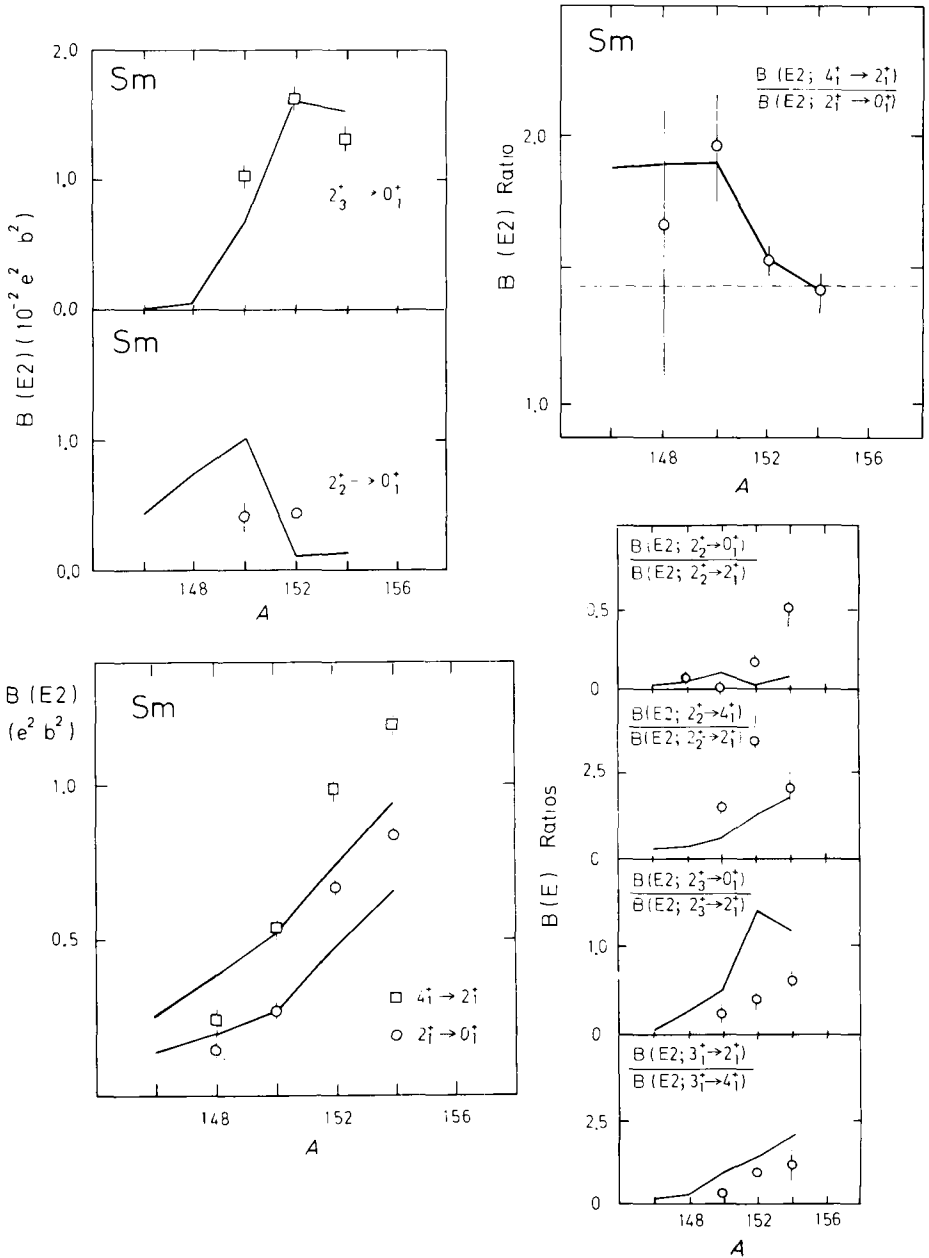


Fig. 8. Theoretical and experimental $B(E2)$ values for the different Sm isotopes.

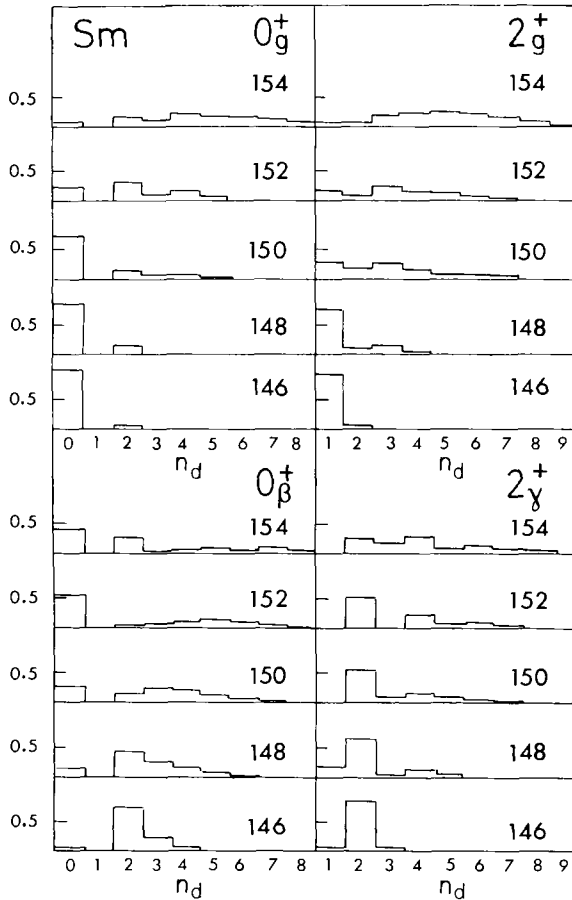


Fig. 9. Anatomy of the wave functions of 0_g^+ , 2_g^+ , 0_β^+ , 2_γ^+ states of the different Sm isotopes according to the components with different number of d-bosons.

While the ground state of ^{148}Sm is a condensate of monopole pairing bosons, the ground state of ^{152}Sm is condensate of quadrupole bosons. Note also the exchange of roles with increasing mass number of the ground state (spherical) and the first excited state (deformed). The two order parameters which measure the interplay between spatial deformations and pairing correlations are the static quadrupole moment and the gap parameter. They are displayed in fig. 10 in comparison with the experimental data. The quantity Q_2 changes by a factor of two in the range of masses $A = 148\text{--}152$.

In the calculation of both the electromagnetic transition probabilities and of the static quadrupole moment one has utilized

$$e_{\text{eff}} = 1.4 e \cdot b. \tag{21}$$

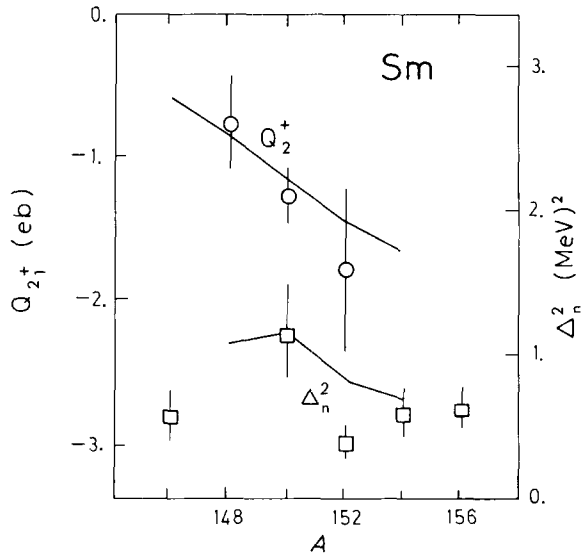


Fig. 10. Theoretical values for the static quadrupole moments and the gap parameters for the different Sm isotopes in comparison with the experimental data.

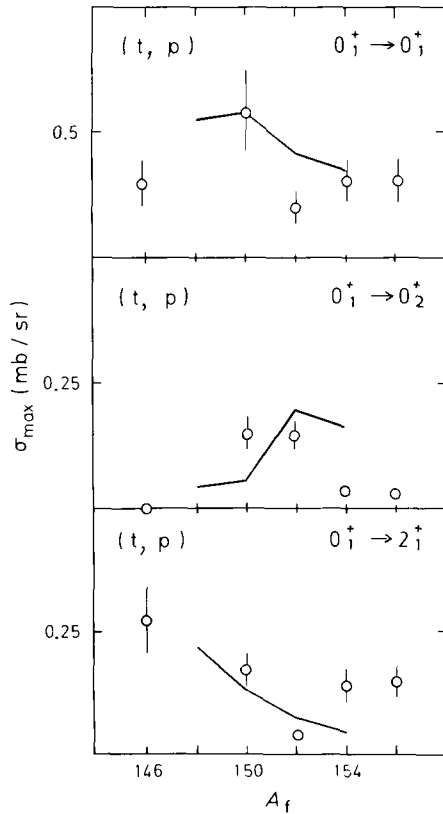


Fig. 11. Comparison between the prediction for the two-neutron transfer probabilities and the (t, p) experimental data (from J. H. Bjerregaard et al., Nucl. Phys. **86** (1966) 145).

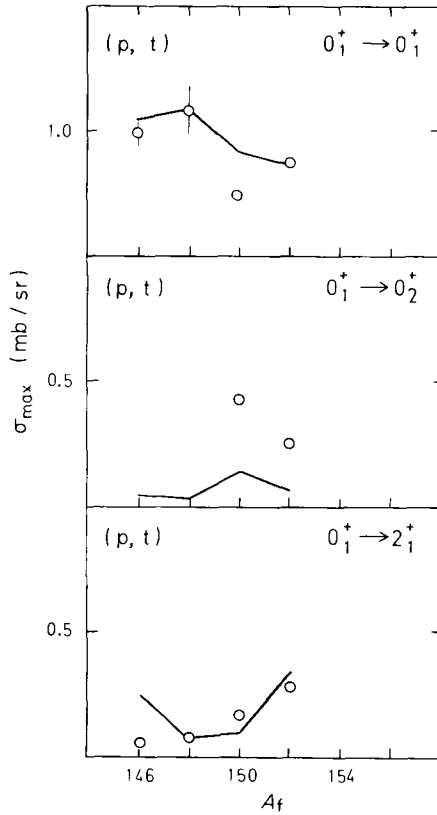


Fig. 12. Comparison between the prediction for the two-neutron transfer probabilities and the (p, t) experimental data (from P. Debenham and N. M. Hintz, Nucl. Phys. **A195** (1972) 385).

Typical values for the single-particle quadrupole matrix element in the Sm isotopes are ~ -0.5 b. The associate effective charge is thus ~ 2.8 which is much larger than the estimated value [cf. eq. (13)]. This result is a consequence that in the model, the core $Z = 50, N = 82$ is assumed to be spherical[†].

In figs. 11 and 12 we display the two-nucleon transfer probabilities predicted by the model in comparison with the experimental data, while in fig. 13 both energy levels and transfer probabilities are collected.

It has been shown³³⁻³⁵) that two-nucleon transfer reactions to the different members of the ground-state rotational band probe, in deformed nuclei, the multipole pairing deformations, that is, the deformations of the Nilsson orbitals close to the Fermi surface. In fact

$$\sigma(\lambda) \approx \left(\sum_v U_v V_v q_v(\lambda) \right)^2 = \left(\frac{A(\lambda)}{G_\lambda} \right)^2, \tag{22}$$

[†] Note also that the predicted sign of Q_0 is opposite to the one observed. This is however a trivial consequence of considering only one type of particle.

where $q_v(\lambda) \sim \langle v || r^\lambda Y_\lambda || v \rangle$ and where U_v, V_v are the BCS occupation parameters. The quantity G_λ is the multipole pairing force [$\sim 27/A$ MeV, cf. ref. ²⁸⁾], and $\Delta(\lambda)$ is the multipole pairing gap. For $\lambda = 0$ we obtain the well-known relation valid for any superfluid system

$$\sigma(\text{g.s.} \rightarrow \text{g.s.}) \approx \left(\frac{\Delta}{G}\right)^2, \tag{23}$$

the quantity $\Delta = \Delta(0)$ being the monopole pairing gap. Note that in a superfluid deformed nucleus, because of the non-conservation of angular momentum, the different multipole pairing correlations give contributions to the monopole pairing gap, leading to a state-dependent pairing gap

$$\Delta_v = G_0 \sum_{v'} U_{v'} V_{v'} + \sum_{\lambda} G_{\lambda} q_v(\lambda) \sum_{v'} U_{v'} V_{v'} q_{v'}(\lambda). \tag{24}$$

The transition between the ground states and to the 2_g^+ member of the ground-state rotational band are well reproduced. Note however the deviations up to ^Q factor of two observed in the (p, t) cross sections to the 2_g^+ states.

Because the $\Delta N = 2$ contributions to the quadrupole pairing gap are very important [cf. refs. ^{33, 34)}] these discrepancies are likely to be associated with having neglected the deformations of the core. The agreement found for the ground-state transitions reflect the correct treatment, in the model, of the monopole pairing degree of freedom.

The 4_g^+ state which is observed with a cross section which is $\sim 3-4\%$ of the ground-state cross section, lies outside the model. For nuclei for which the hexadecapole term in the Nilsson potential becomes important, the transition to the 4^+ state can become as large as 30% of the ground-state cross section ³⁶⁾. In these cases the need to allow pairs of particles to couple to $\lambda = 4$ (g-bosons) becomes obvious.

Of the 0^+ states which aside from the ground state are strongly excited in two-nucleon transfer reactions, the model predicts only one. Even for the one predicted, the observed cross section is about a factor of two larger than predicted. This may be due to the fact that the model does not contain the degree of freedom associated with pairing vibrations which are specifically excited in two-nucleon transfer reactions. In this case, the large change of the shell structure which gives rise to two minima in the potential energy surface, leads to large fluctuations in the gap and in the shape degrees of freedom, and the associated modes mix strongly.

The coupling between pairing and β -vibrations has been studied [cf. e.g. ref. ³⁷⁾] by diagonalizing the pairing-plus-quadrupole hamiltonian in a Nilsson-plus-BCS basis, making use of the RPA. The properties of the $K = 0$ vibrations are determined by the solutions of the dispersion relation

$$\begin{vmatrix} A & D & E \\ DW_j^2 & B & F \\ EW_j^2 & F & C - \frac{1}{2}K \end{vmatrix} = 0, \tag{25}$$

where

$$\begin{aligned}
 A &\equiv \sum_i \frac{E_i g_i}{E_i^2 - W_j^2} - \frac{1}{G}, & D &\equiv \sum_i \frac{f_i}{E_i^2 - W_j^2}, \\
 B &\equiv \sum_i \frac{E_i f_i^2}{E_i^2 - W_j^2} - \frac{1}{G}, & E &\equiv \sum_i \frac{q_i g_i}{E_i^2 - W_j^2}, \\
 C &\equiv \sum_i \frac{E_i^2 q_i^2}{E_i^2 - W_j^2}, & F &\equiv \sum_i \frac{E_i q_i f_i}{E_i^2 - W_j^2},
 \end{aligned} \tag{26}$$

and

$$\begin{aligned}
 g_i &\equiv \delta(v, \omega), & f_i &\equiv (U_v^2 - V_v^2) \delta(v, \omega), \\
 q_i &\equiv q_{v\omega} (U_v V_\omega + U_\omega V_v), & E_i &= E_v + E_\omega.
 \end{aligned} \tag{27}$$

The quantities U_v and V_v are the BCS occupation parameters associated with the Nilsson orbital v , while $q_{v\omega}$ stands for the matrix element $\langle v | r^2 Y_{20} | \omega \rangle$. The quantity E_v is the quasiparticle energy associated with the energy it takes to break a pair in the Nilsson orbital v .

There are two fields associated with the pairing modes and one with the β -vibrations. They are proportional to $U^2 + V^2$ and $U^2 - V^2$ and to $UV + VU$, respectively. The fluctuations of the fields $U^2 + V^2$ and $U^2 - V^2$ give rise to the spurious state associated with the variation of the number of particles and to vibrations of the pairing gap (pairing vibrations). The dispersion relation $A = 0$ together with the gap equation is equivalent to the BCS gap equation, while $B = 0$ leads to a coherent two-quasi-particle state based on 2p-2h types of excitations [cf. e.g. ref. ¹³]. The fluctuations of the field $UV + VU$ lead to a coherent two-quasiparticle excitation based on the particle-hole like excitation whose transition density is concentrated on the nuclear surface. These vibrations can be viewed as quadrupole surface oscillations which conserve axial symmetry.

The reason why a mode generated by the quadrupole degree of freedom (1p-1h, $\lambda = 2$) can mix with a mode generated by the monopole pairing degree of freedom (2p-2h, $\lambda = 0$) is because in deformed nuclei both the number of particles and the angular momentum are violated in the intrinsic state. The coupling between the pairing and β -vibrations is governed by the term F which may lead to contributions of the same order of magnitude as the diagonal contributions which are controlled by B and C .

It is noted that the pairing vibration is not an intruder state [cf. ref. ³⁸] in a system in which pairing correlations are important, but the expression of the quantal fluctuations of the average pairing field. It is also noted that the breaking of gauge invariance (i.e. violation of the number of particles) is at the basis of the collective properties of this degree of freedom, in a similar way as the breaking of rotational invariance (i.e. non-conservation of the angular momentum), is at the basis of the rotational spectra in normal space.

Note also that the detailed mechanism by which pairing vibrations can become strongly excited will depend on the interplay between pairing and quadrupole correlations and shell structure. In particular, the value of the gap (24) associated with low-lying two-quasiparticle states, will depend on the relative sign of the single-particle quadrupole moment $q_{\nu}(2)$ of the Nilsson levels around the Fermi surface, which determines $\sum_{\nu} U_{\nu} V_{\nu} q_{\nu}(2)$ and the sign of $q_{\nu}(2)$ associated with single-particle levels ~ 0.5 MeV away from the Fermi surface. If $q_{\nu}(2)$ has opposite sign (oblate) to the average sign of $q_{\nu}(2)$ (prolate), it can result in a gap $\Delta_{\nu} \sim 0$. This mechanism thus gives rise to excited 0^+ pairing vibrations (two-quasiparticle states) associated with fluctuations of a gap which is very small. Some of these states will thus be populated with a cross section of the order of 20–30 % of the ground-state cross section. A different behaviour is also expected for (t, p) and (p, t), depending on whether the oblate orbitals are below ($U_{\nu}^2 \approx 0$) or above ($U_{\nu}^2 \approx 1$) the Fermi surface. This type of 0^+ states have been observed in some actinide isotopes [cf. ref. ³⁵] and references therein; cf. also ref. ³⁹].

A pairing vibration can also be strongly populated if its main two-quasiparticle component is based on a “hot orbital”, i.e., an orbital which displays a strong two-nucleon transfer cross section, which in general is about one order of magnitude larger than that associated with neighbouring orbitals. Subshell closures will also strongly affect the cross section associated with low-lying pairing and β -vibrations. [cf. ref. ³⁴] and refs. therein].

This rich pattern will require the introduction of many different s' -bosons in the IBM, as many degrees of freedom are responsible for the occurrence of strongly excited two-nucleon transfer states with $J^{\pi} = 0^+$

5. Conclusions

As usual, it is difficult to assess the validity of a model from the study of schematic versions of it or from a comparison to the experimental data. In the first case the objection that can be raised is, to what extent the schematic model contains the essential features which one is trying to check. In the second case, whether the discrepancies observed cannot be eliminated by simple extensions of the model.

In any case, a description of the nuclear spectrum in terms of pairs of fermion coupled to 0^+ and to 2^+ and moving in a single j -shell, seems to lead to γ -bands in deformed nuclei which are too close to the spherical, vibrational pattern.

It fails in the description of β -bands almost totally. In fact, because of the central role played by the degrees of freedom of the shell structure, and by the pairing vibrations which mix strongly with the β -vibrations, the eventual success or failure of the model concerning the properties of the β -band are not too relevant. The model does not contain the associated degrees of freedom and a series of s' -bosons (pairing vibrations, pairing isomers, “hot” two-quasiparticle orbitals, etc.), have to be introduced to get a detailed description of the nuclear spectrum of deformed nuclei.

Concerning the ground-state band, departures of about a factor of two are observed in the (t, p) cross sections associated with the 2_g^+ , and the cross section associated with the 4_g^+ is zero. Because the hexadecapole deformation can play an important role in (t, p) processes, a g-boson may be needed in many cases not only to account for the 4^+ cross section, but because of the renormalization effect it has on the 2^+ cross section.

The cut-off which the model has due to the finite space is only a limitation, which has to be removed if a detailed comparison with the high-spin states ($I \gtrsim 8^+$) is to be carried out.

In spite of all these limitations, the simplicity brought by the quadrupole boson model and by the IBM can be attractive. An example of why this should be is provided by the change in the spectrum and in the structure of the wave functions associated with the phase transition taking place around ^{150}Sm .

References

- 1) L. D. Landau, J. Phys. USSR **5** (1941) 1;
L. D. Landau and E. M. Lifshitz, Statistical physics (Pergamon, London, 1958)
- 2) H. Fröhlich, H. Pelzer and S. Zienau, Phil. Mag. **41** (1950) 221
- 3) T. D. Lee and D. Pines, Phys. Rev. **88** (1952) 960;
D. Pines, Elementary excitation in solids (Benjamin, New York, 1963)
- 4) W. Kohn, Phys. Rev. **105** (1957) 509; J. M. Luttinger, Phys. Rev. **119** (1960) 1153
- 5) A. B. Migdal, Theory of finite fermi systems and applications to atomic nuclei (Interscience, New York, 1967);
A. R. Abrikosov, L. P. Gor'kov and I. E. Dzyaloshenski, Methods of quantum field theory in statistical physics (Prentice Hall, 1963)
- 6) A. Bohr and B. R. Mottelson, Nuclear structure vol. II (Addison-Wesley, Reading, Mass., 1975)
- 7) D. R. Bès, G. G. Dussel, R. A. Broglia, R. Liotta and B. R. Mottelson, Phys. Lett. **52B** (1974) 253;
D. R. Bès, R. A. Broglia, G. G. Dussel, R. J. Liotta and H. Sofia, Nucl. Phys. **A260** (1976) 1, 27;
D. R. Bès, R. A. Broglia, G. G. Dussel and R. Liotta, Phys. Lett. **56B** (1975) 109
- 8) D. R. Bès, R. A. Broglia, G. G. Dussel, R. Liotta and R. Perazzo, Nucl. Phys. **A260** (1976) 77;
D. R. Bès and R. A. Broglia, Topical Conf. on problems of vibrational nuclei, Zagreb, Sept. 1974, ed. G. Alaga, V. Paar and L. Šips (North-Holland, Amsterdam, 1975) p. 1
- 9) P. F. Bortignon, R. A. Broglia, D. R. Bès and R. Liotta, Phys. Reports **30C** (1977) 305
- 10) M. G. Mayer and J. H. D. Jensen, Elementary theory of nuclear shell structure (Wiley, New York, 1955)
- 11) A. Bohr and B. R. Mottelson, Mat. Fys. Medd. Dan. Vid. Selsk. **27**, no. 16 (1953)
- 12) A. Bohr, Compt. Rend. Congres Int. de Physique Nucléaire, Paris, 1964, vol. 1 (Ed. Centre National de la Recherche Scientifique, Paris, 1964) p. 487
- 13) D. R. Bès and R. A. Broglia, Nucl. Phys. **80** (1965) 289;
R. A. Broglia, in Proc. Eleventh Summer Meeting of nuclear physicists, Herceg Novi, ed. L. Šips (Nuclear Energy Commission of Yugoslavia, 1966) vol. 1, p. 201
- 14) D. Janssen, R. V. Jolos and F. Döna, Nucl. Phys. **A224** (1974) 43;
R. V. Jolos, F. Döna and D. Janssen, Yad. Fiz. **20** (1974) 310; JINR P4-7223 Dubna, 1973; TMF **20** (1974) 112;
D. Janssen, Problems of vibrational nuclei, ed. G. Alaga, V. Paar and L. Šips (North-Holland, Amsterdam, 1975) p. 75
- 15) F. Iachello, in Interacting bosons in nuclear physics, ed. F. Iachello (Plenum, New York, 1979) p. 1 and references therein;
A. Arima, *ibid.* p. 179
- 16) T. Otsuka, A. Arima, F. Iachello and J. Talmi, Phys. Lett. **76B** (1978) 139; **66B** (1977) 205

- 17) T. Otsuka, A. Arima and F. Iachello, Nucl. Phys. **A309** (1978) 1
- 18) D. R. Bès and R. A. Broglia, in *Interacting bosons in nuclear physics*, ed. F. Iachello (Plenum, NY, 1979) p. 143
- 19) R. A. Broglia, K. Matsuyanagi, H. Sofia and A. Vitturi, Nucl. Phys. **A348** (1980) 237
- 20) P. F. Bortignon, R. A. Broglia and D. R. Bès, Phys. Lett. **76B** (1978) 153
- 21) T. Otsuka, in *Interacting bosons in nuclear physics*, ed. F. Iachello (Plenum, New York, 1979) p. 93; J. B. Mc Grory, *ibid.* p. 121
- 22) F. Sakata, private communication
- 23) A. Bohr and B. R. Mottelson, Phys. Scripta, **22** (1980) 468
- 24) R. A. Broglia, Invited talk to the Workshop on Interacting Bose-Fermi systems in nuclei, Erice, June 12–19, 1980
- 25) D. R. Bès, R. A. Broglia, E. Maglione and A. Vitturi, Nucl. Phys., to be published
- 26) A. Gelberg and U. Kaup, in *Interacting bosons in nuclear physics*, ed. F. Iachello (Plenum, NY, 1979) p. 59; Z. Phys. **A293** (1979) 311
- 27) O. Scholten, in *Interacting bosons in nuclear physics* ed. F. Iachello (Plenum, NY, 1979) p. 17; O. Scholten, F. Iachello and A. Arima, Ann. of Phys. **115** (1978) 325; A. Saha, O. Scholten, D. C. J. M. Hageman and H. T. Fortune, Phys. Lett. **85B** (1979) 215
- 28) D. R. Bès, R. A. Broglia and B. Nilsson, Phys. Lett. **50B** (1974) 213
- 29) D. R. Bès, R. A. Broglia and B. Nilsson, Phys. Reports **16C** (1975) 1
- 30) R. A. Broglia, V. Paar and D. R. Bès, Phys. Lett. **37B** (1971) 257
- 31) D. Schwalm, GSI preprint 80–26, December 1980
- 32) O. Scholten, The interacting boson approximation model and applications, thesis, University of Groningen (1980) unpublished
- 33) R. A. Broglia, C. Riedel and T. Udagawa, Nucl. Phys. **A135** (1969) 561
- 34) R. A. Broglia, O. Hansen and C. Riedel, *Advances in nuclear physics*, vol. 6 (1973) p. 287
- 35) I. Ragnarsson and R. A. Broglia, Nucl. Phys. **A263** (1976) 315
- 36) K. Kubo, R. A. Broglia, C. Riedel and T. Udagawa, Phys. Lett. **32B** (1970) 29
- 37) D. R. Bès, Nucl. Phys. **49** (1963) 544
- 38) KVI Report (1979) p. 101
- 39) J. Jänecke, F. D. Becchetti, D. Overway, J. D. Cossairt and R. L. Spross, Phys. Rev. **C23** (1981) 101